Sensors and Actuators A 317 (2021) 112474

Contents lists available at ScienceDirect

Sensors and Actuators A: Physical

journal homepage: www.elsevier.com/locate/sna

# Wet oxidation of 3C-SiC on Si for MEMS processing and use in harsh environments: Effects of the film thicknesses, crystalline orientations, and growth temperatures

Tuan Anh Pham [a,*], Leonie Hold [a], Alan Iacopi [a], Tuan-Khoa Nguyen [a], Han Hao Cheng [b], Toan Dinh [a,c], Dzung Viet Dao [a,d], Hang Thu Ta [a,e,f], Nam-Trung Nguyen [a,*], Hoang-Phuong Phan [a,*]

[a] Queensland Micro and Nanotechnology Centre, Griffith University, QLD, Australia
[b] Centre for Microscopy and Microanalysis, The University of Queensland, QLD, Australia
[c] School of Mechanical and Electrical Engineering, University of Southern Queensland, QLD, Australia
[d] School of Engineering and Built Environment, Griffith University, Australia
[e] School of Environment and Science, Griffith University, Australia
[f] Australian Institute for Bioengineering and Nanotechnology, University of Queensland, QLD, Australia

ARTICLE INFO

*Article history:*
Received 18 August 2020
Received in revised form
22 November 2020
Accepted 23 November 2020
Available online 26 November 2020

*Keywords:*
MEMS
Wet oxidation
Silicon carbide
Epitaxial growth
Harsh environments

ABSTRACT

An in-depth understanding of the formation of silicon dioxide ($SiO_2$) on silicon carbide (SiC) in thermal oxidation is imperative for micro/nano fabrication processes, integration of electronic components, and evaluation of SiC device performance under extreme conditions. Herein, we report a comprehensive study on the effects of crystalline orientations, thicknesses, and growth temperatures of cubic SiC films on their wet oxidation properties. The oxidation rate and surface morphology were characterized using atomic force microscopy (AFM) and light reflectance measurement systems. Our experimental results revealed the role of defects in the SiC crystal on the oxidation that relates to SiC thickness, deposition conditions, crystal orientation and temperature of wet oxidation. Critically, the electrical properties of SiC films oxidized at 900 °C remained the same as the unoxidized film as confirmed by room-temperature current-voltage measurements, indicating a long-term service temperature of SiC. These findings are expected to provide crucial information on the effects of defects on the formation of $SiO_2$ on SiC films at different oxidation temperatures, which is highly essential for establishing a basic platform for the fabrication of high-performance SiC-based electronic devices.



## 1. Introduction

Silicon carbide (SiC) is emerging as an ideal candidate for micro-electromechanical system (MEMS) devices operating in extreme conditions such as elevated temperature, radiation, and chemically harsh environments thanks to its remarkable properties [1–5]. In particular, the chemical inertness of SiC against several liquid electrolytes offers the reliable and long-term operation, while their large energy gap, good thermal conductivity, high breakdown voltage and excellent mechanical strength allow for unique functionalities as well as high-temperature operations that cannot be achieved with the conventional Si technology. One of the major merits of SiC over other non-silicon wide bandgap semiconductors (e.g. GaN or diamond) is its ability to be thermally oxidized to $SiO_2$, which is very promising for its use as a gate dielectric in transistors, an insulator to isolate electronic components in integrated circuits or a sacrificial layer in nano-machining [6–8]. In this regard, high quality oxide growth of SiC in a dry environment is routinely done at very high temperatures ~1250 °C for MOSFET fabrication [52]. To date, a considerable number of studies have been devoted to a better understanding of the oxidation mechanism and behavior of SiC via various oxidation processes [9–13]. The well-established thermal oxidation mechanism of Si has been exploited to investigate the oxidation mechanism of SiC under similar oxidation parameters. For example, Kakubari et al. performed real-time observation of SiC thermal oxidation using an *in-situ* ellipsometer and found that the oxidation-time dependence of $SiO_2$ thickness can be interpreted

* Corresponding authors.
*E-mail addresses:* tuananh.pham2@griffithuni.edu.au (T.A. Pham), nam-trung.nguyen@griffith.edu.au (N.-T. Nguyen), h.phan@griffith.edu.au (H.-P. Phan).

https://doi.org/10.1016/j.sna.2020.112474
0924-4247/

**Table 1**
List of different SiC films epitaxially grown on a Si substrate employed for wet oxidation.

| Sample | Thickness (nm) | Deposition temperature | Crystalline orientation |
|---|---|---|---|
| S1 | 89 | 1000 °C | <100> |
| S2 | 389 | 1000 °C | <100> |
| S3 | 394 | 1000 °C | <111> |
| S4 | 403 | 1250 °C | <111> |
| S5 | 400 | 1250 °C | <100> |
| S6 | 976 | 1250 °C | <100> |

Low temperature: 1000 °C.
High temperature: 1250 °C.

using the Deal-Grove model, similar to Si oxidation [14]. Song et al. modified Deal-Grove model by taking the carbon oxidation process into account and concluded that a linear-parabolic formula can be applied to SiC oxidation [15]. Similarly, Narushima et al. studied the oxidation of chemically vapor-deposited SiC in wet oxygen using a thermogravimetric technique and demonstrated that the oxidation kinetics follow a linear-parabolic relationship over the temperature range of 1823 to 1923 K [16]. The influence of crystal orientation on the oxidation of SiC has attracted a great attention. While the oxidation of different crystalline orientations for Si such as <111> and <100> is well characterized and modeled, the oxidation of SiC on Si is more complicated. This process relies on the inward diffusion of oxygen and ultimately the out diffusion of carbon from an imperfect lattice. SiC on Si has stacking faults that reduce in density away from the Si interface. SiC crystal orientation is derived from that of Si during the heteroepitaxial SiC deposition where the lattice mismatch is ~20 %; however, there are many domains created on the surface which represent another crystal imperfection [18,19]. A recent study by Simonka et al. reported that SiC exhibits an anisotropic oxidation nature, where the oxidation growth rates depend strongly on the crystalline orientation of the SiC crystal [20].

On the other hand, wet oxidation of SiC, like Si, provides a higher oxide growth rate than dry $O_2$ oxidation and so is regarded as a far harsher environment. However, wet oxidation usually does not provide the highest quality device gate oxides because of a lower-density oxide and dielectric strength of the oxide layers compared to that formed by dry oxidation. This leads to the fact that the formation of the oxide layers on SiC in a humid environment is highly undesired in some cases due to the as-grown oxide layers may negatively impact on the working performance of SiC-based electronic devices operating at elevated temperatures. Therefore, more research efforts in this context are urgently needed to achieve a better understanding of the influence of wet oxidation on SiC, which will be helpful in improving and optimizing the working performance of high-quality SiC-based electronic devices. However, to the best of our knowledge, comprehensive studies focused on the influence of the crystalline orientation, thickness, and growth temperature of SiC films on the wet oxidation of SiC are extremely rare [17,21,22].

Herein, we report a comprehensive study on the effects of the crystalline orientation, thickness, and growth temperature of SiC films on wet oxidation of SiC films grown on Si substrates with respect to different oxidation temperatures using AFM and light reflectance thin film thickness measurement. In particular, we examined six different SiC films, which were epitaxially grown on Si substrates at different growth temperatures. The crystalline orientation of these SiC films is either <100> or <111> oriented surface and their thicknesses vary from 89 nm to 976 nm (Table 1). Our experimental results revealed that the oxidation of epitaxial 3C-SiC depends on several factors such as deposition temperature, oxidation temperature, crystal orientation and film thickness. In particular, the thinner the SiC film, the higher the average oxidation rate under the same crystalline orientations and growth temperatures of SiC films. On the other hand, the average oxidation rate appears to be higher on <111> oriented and low-temperature grown SiC films compared to that of <100> oriented and high-temperature grown ones. Importantly, our AFM data pointed out that the defects strongly influence the wet oxidation rate, which is dependent on the film thicknesses, crystalline orientations, and growth temperature. These findings are expected to significantly contribute to the current understanding of the behavior of wet oxidation of SiC, and thus helping in the evaluation the performance of different oxidized SiC films as a function of oxidation temperature, which can be considered as a stepping-stone for an effective and reliable production of the next generation SiC-based electronic devices.

## 2. Experimental

### 2.1. Epitaxial deposition of SiC films on Si substrates

Unintentionally doped 3C-SiC films at different thicknesses and crystalline orientations were grown on on-axis 150 mm dia. Si substrates in an SPT Microtechnologies USA Epiflx reactor. The Epiflx reactor was designed for large batch epitaxial deposition of 3C SiC on wafers upto 300 mm in diameter. Si substrates were cleaned using the standard Radio Corporation of America (RCA) cleaning procedures prior to being loaded into the reactor. SiC films were deposited at either 1000 °C or 1250 °C by an Alternative Supply Epitaxy method previously described elsewhere [45,46]. Compared with the conventional continuous supply epitaxy deposition method, the ASE method provides a significant reduction in crystal defects for a given temperature. The resulting films were close to atomically smooth and did not suffer from Si voiding under the film that leads to additional SiC crystal defectivity.

### 2.2. Wet-oxidation of epitaxially deposited SiC films

The wet oxidation of SiC was performed using a semiconductor type diffusion furnace from HiTech Furnaces UK. Water vapor was generated by bubbling nitrogen as a carrier gas through water at 96 °C. Precise control of the vapor partial pressure and temperature was achieved over wet oxidation at temperature of 900, 950, 1000 and 1050 +/−0.5 °C for a period of 10 h. Detailed process flow of the ramping-up, stabilization, post-annealing, cooling-down and wet oxidation period is shown in Scheme 1.

### 2.3. Material characterizations

The thicknesses of SiC films were measured using thin film reflectance measurement using a Nanometrics Nanospec/AFT 210, assuming a consistent refractive index of 2.65. Spectral reflectance curves were obtained by the surface profilometry technique using Filmetric F40. The surface topography of SiC films was characterized using Atomic Force Microscope (AFM) ParkAFM NX20 operating in air non-contact mode and using a cantilever tip of < 10 nm. To determine the thickness of the as-grown $SiO_2$ using AFM, the SiC films were patterned by a standard photolithography process, followed by a buffered oxide etching (BOE) to remove the exposed as-grown oxide layers. The current-voltage ($I$–$V$) characteristics of the SiC films before and after oxidation were obtained at room temperature using a semiconductor device parameter analyzer (Agilent B1500). Before the measurements, a thin layer of aluminum was deposited on the films by sputtering and subsequently patterned to form metal electrodes. The quality of the Aluminum was assessed by measuring the relative reflectance to Si at 436 and 480 nm at

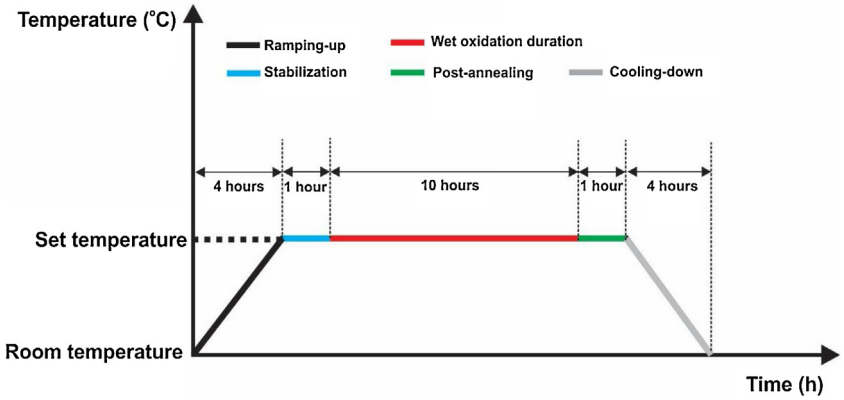


**Scheme 1.** Detailed process flow of the wet oxidation of SiC performed in this study.

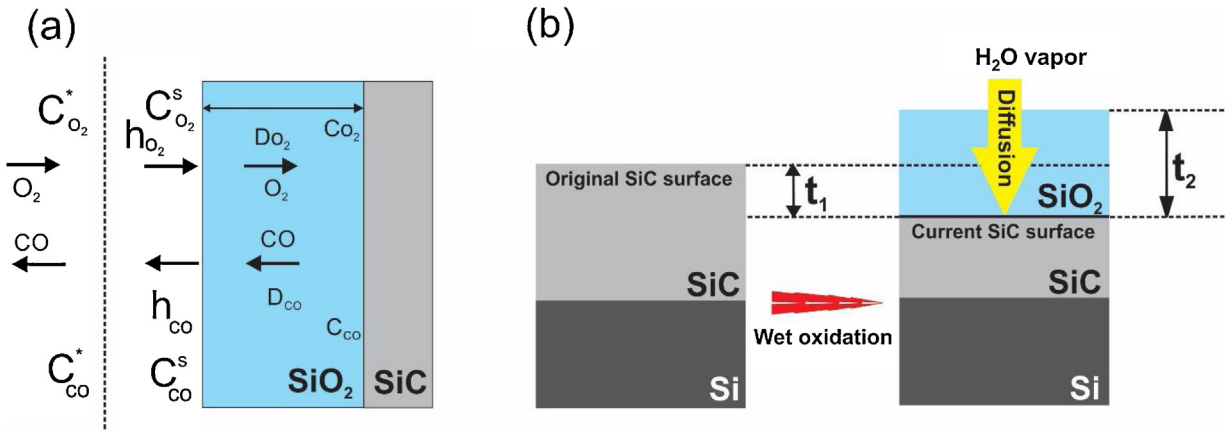


**Fig. 1.** (a) Five steps for oxidation of SiC proposed by Song and co-workers [15] and (b) the concept of wet oxidation in SiC films epitaxially grown on a Si wafer.

>218 % and >235 % respectively that confirms metal reflectivity is of semiconductor industry quality.

## 3. Results and discussion

According to previous studies, the oxidation mechanism of SiC films can be described using the same model for the thermal oxidation of Si proposed by Deal and Grove with some modifications [23–26]. In particular, the growth in the three-step thermal oxidation of Si follows the following reaction: $X^2 + AX = B(t + \tau)$, where $X$ stands for the thickness of the oxide, $t$ is the oxidation time, the quantity $\tau$ corresponds to a shift in the time coordinate, which corrects for the presence of the initial oxide layer. $B$ and $B/A$ are parabolic and linear rate constant, respectively. However, it is impossible to directly apply Deal and Grove model for the oxidation of SiC because this model does not include the gas out-diffusion. Song et al. proposed a five-step oxidation process for SiC, in which gas out-diffusion of the product during the thermal oxidation was taken into account as shown in Fig. 1**a**. As such, this five-step dry-oxidation process of SiC is considerably more complicated than the three-step oxidation process of Si as following [15,23]. These steps include (i) a flux of oxidant species arriving at the oxide surface; (ii) in-diffusion of oxidant species through the oxide film; (iii) reaction with SiC at the $SiO_2$/SiC interface; (iv) out-diffusion of product gases through the oxide film; and (v) removal of product gases away from the oxide surface.

For SiC, the last two steps are not involved in the oxidation of Si. Moreover, the authors suggested that oxidation rate of SiC is about one order of magnitude slower than that of Si under similar oxidation conditions. The first and last steps of this oxidation process are rapid, and thus are not rate-controlling steps [15]. Based on these findings, we assumed that wet oxidation of SiC can also be described by the five-step model for SiC dry oxidation mentioned above. Fig. 1 shows the basic process for wet oxidation of SiC films epitaxially deposited on a Si substrate. It is imperative that oxidants must diffuse across the newly formed oxide layer and subsequently react with SiC at the $SiO_2$/SiC interface for successive oxidation. In the wet oxidation process, water ($H_2O$) molecules instead of oxygen ($O_2$) molecules are the oxidants, which dissociate at high temperature to form hydroxide (HO) before reaching the SiC surface. More importantly, hydroxide exhibits faster diffusion mobility in SiC than pure $O_2$ which results in a higher oxidation rate of wet oxidation than dry oxidation, similar to the case of Si [47]. We proposed that wet oxidation of SiC consists of the consumption of SiC (marked as $t_1$ in Fig. 1), the formation of $SiO_2$ layers (marked as $t_2$ in Fig. 1) and the removal of excess C in various forms of gases (not marked), which is governed by the following reactions:

$$SiC(s) + 3H_2O(g) \rightarrow SiO_2(s) + 3H_2(g) + CO(g)$$

$$SiC(s) + 4H_2O(g) \rightarrow SiO_2(s) + 4H_2(g) + CO_2(g)$$

Fig. 2**a** presents the color chart of three different SiC films with respect to the variation in thicknesses and oxidation temperatures, observed by naked eye. Apparently, the SiC films showed different colors at different thickness [27]. Only a slightly gradual change was observed in the colors of the SiC films wet-oxidized at 900, 950 and 1000 °C with respect to the unoxidized ones. However, the colors change was significant for films oxidized at 1050 °C. These results are consistent with the absorption spectra, where a slight change was measured as the oxidation temperature increased from 900

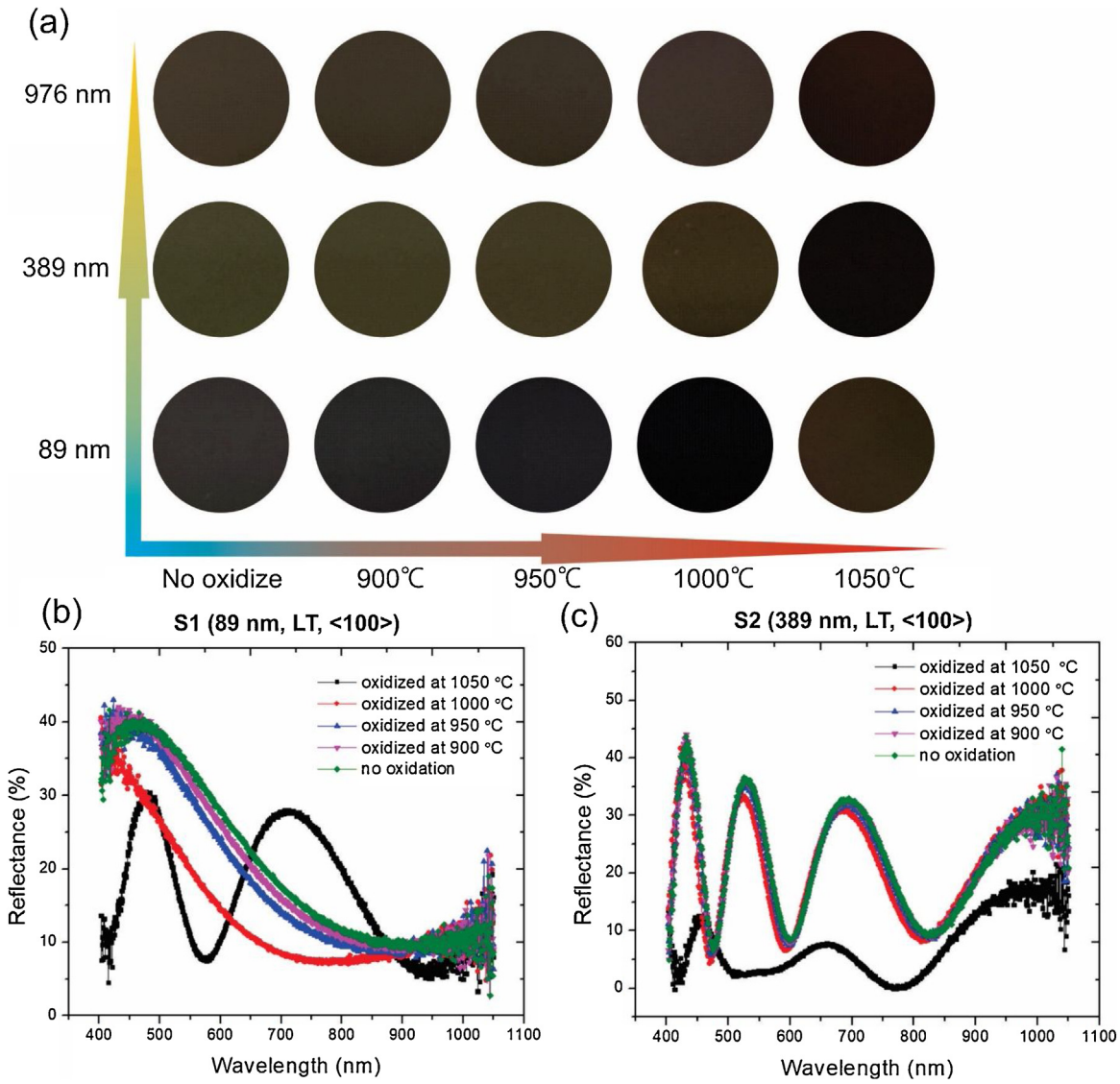


**Fig. 2.** Optical characterization of the oxidized SiC film. (a) Photograph taken under normal daylight conditions of three different SiC films, showing the color variation with respect to the changes in the SiC thicknesses and the growth of oxide layers. (b) Spectral reflectance curves of SiC films having different thicknesses, revealing the changes of adsorption features as oxidation temperatures increased.

°C to 1000 °C (Fig. 2b), while a huge shift was found for the films oxidized at 1050 °C (Fig. 2c). As expected, wet oxidation in 3C-SiC is a highly temperature dependent process.

As mentioned above, $SiO_2$ is usually grown by the reaction of SiC with the oxidant ($H_2O$), where the thickness of the as-grown oxide layer is typically larger than that of the consumed SiC film (i.e. $t_2 > t_1$, Fig. 1). Fig. 3 plots the thickness of the as-grown $SiO_2$ as a function of oxidation temperature (the measurement data can be found in **Table S1 to S4**). Accordingly, the thickness of the oxide layers in all samples increased as oxidation temperature increased from 900 °C to 1050 °C. This is reasonable as the diffusivity of oxidant species through the as-grown oxide layer strongly depends on temperature following an Arrhenius-type equation, $D \propto \exp[-E_A/RT]$, where

$D$ is the diffusion coefficient, $E_A$ is the activation energy, and $R$ is the gas constant. Notably, the thickness of the as-grown $SiO_2$ observed in the oxidation temperate ranging from 900 to 1000°C is relatively small compared to that observed at 1050 °C for all examined SiC films. For the SiC films with the same thickness (~394 nm) and being grown at a low LPCVD temperature, the <111> oriented SiC film exhibits a considerably thicker oxide layer than the <100> SiC film (189 nm and 91 nm at 1050 °C of oxidation, respectively). This result implies a significant crystallographic orientation effect on the wet oxidation process of SiC (Fig. 3b).

This phenomenon could be related to the differences in the densities of SiC units between <111> and <100> surfaces. Having a larger number of SiC units on the <111> surface that can take part in the chemical reactions to form $SiO_2$ will lead to a faster oxidation growth, similar to the case of Si [19]. Another possible reason is the high density of stacking fault defects in <111> film compared to the <100> film, as previously confirmed by our TEM measurements [48]. Interestingly, the crystallographic orientation effects on the wet oxidation is less profound for SiC films deposited at high LPCVD temperature (Fig. 3c). This result implies that wet oxidation growth of epitaxial SiC films depends on crystal defectivity. Higher SiC deposition temperature generally leads to less crystal defects for a give film thickness. To further prove this finding, we compared two <111> SiC films having the same thickness but being LPCVD grown at different temperatures (Fig. 3d). Evidently, the low-temperature LPCVD films experienced a significantly oxidation rate than the high-temperature LPCVD ones (189 nm and 87 nm at 1050 °C of wet oxidation, respectively). This feature can be associated with a high density of defects in thin films epitaxially grown

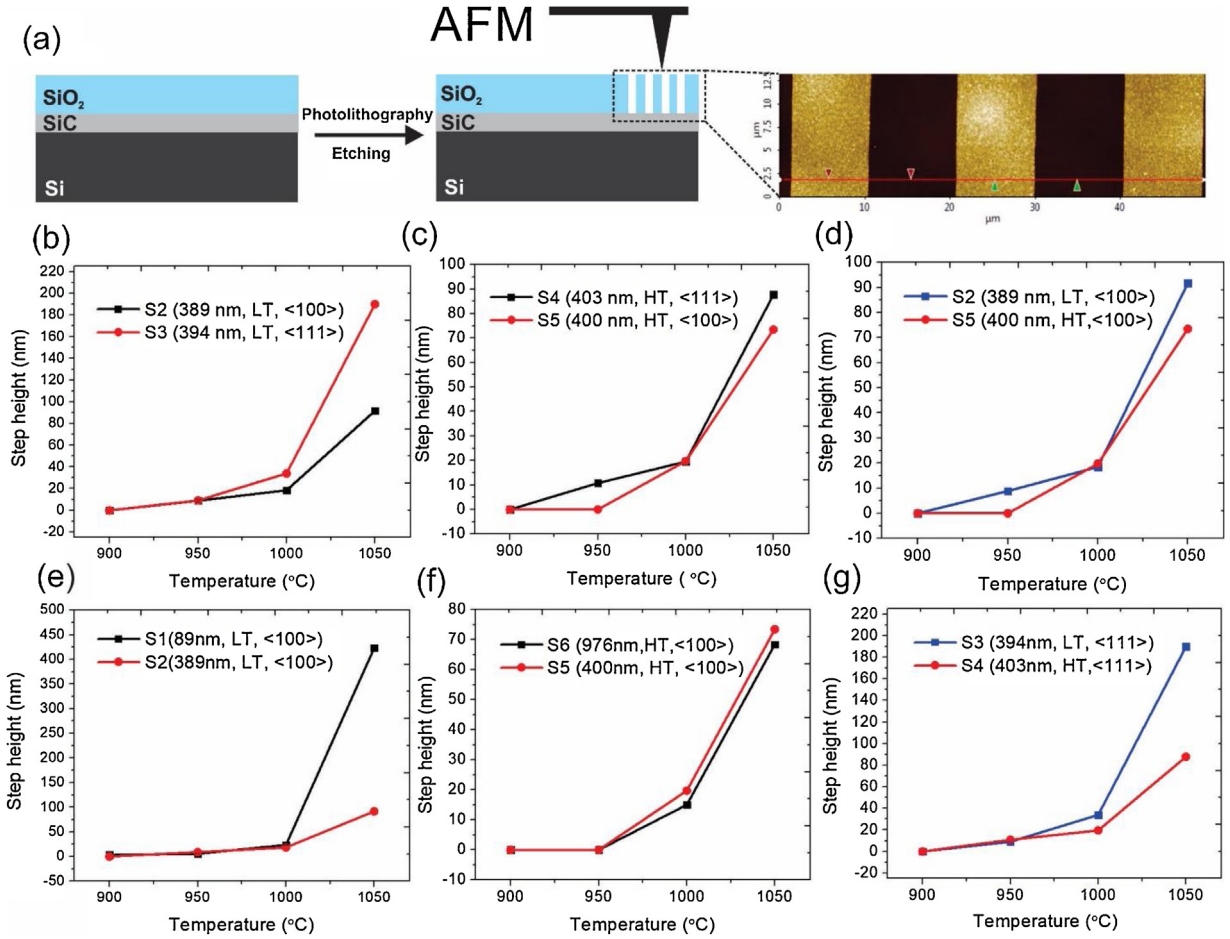


**Fig. 3.** (a) Schematic illustration of the patterning process for AFM measurements and an example of AFM image used to determine the thickness of the SiO2 layer. (b) to (g) The dependence of the as-grown $SiO_2$ thickness on the SiC thicknesses, crystalline orientations, and growth temperature of SiC films with respect to oxidation temperature ranging from 900 °C to 1050 °C.

on a foreign substrates at low temperature, such as misfit dislocations, stacking faults, twin boundaries, or steps and kinks, which are usually found in SiC as well as other semiconductors [28–31]. It was previously reported that these surface defect sites are more chemically active compared to defect-free (or less defective) surface sites [32–34,51]. Moreover, surface defects such as vacancies and pinholes can facilitate the infiltration of oxidant species into the inside layers of SiC and thus, rapidly generate the chemical reactions of the wet oxidation [35,36]. Therefore, a higher density of the surface defect sites in the low-temperature LPCVD films results in a thicker $SiO_2$ layer than that of the high-temperature LPCVD films. Notably, the influence of LPCVD temperature in the oxidation is more visible in the <111> films than the <100> films and therefore, further confirming the anisotropic oxidation nature of SiC (Fig. 3e).

Another important feature that could contribute to the oxidation rate of SiC is the thickness of the film, as this parameter correlates to the defect density [49,50]. The experimental data indicates that the 89-nm-thick SiC film exhibits a more significant oxidation rate than the 389-nm-thick SiC film (Fig. 3e). In particular, at 1050 °C, the thickness of the as-grown oxide of the 89-nm-thick SiC sample was found to be 430 nm, almost five times larger than that of the unoxidized SiC films. This markedly thick oxide layer suggests that the oxidation process not only occurred in the thin SiC film but also taken place in the Si substrate underneath. This possibility is strongly supported by the fact that the oxidation rate of Si is much higher than that of SiC. On the other hand, for thicker SiC films (e.g. 400 nm and 976 nm), no remarkable difference was observed in the oxidation rate (Fig. 3g).

Fig. 4**a** shows the oxidation rates (i.e. $t_{SiO2}$/time) of all examined SiC films as a function of oxidation temperature. Apparently, the differences in the oxidation rates of all the films are relatively small in the oxidation temperature ranging from 900 to 1000 °C, but become more visible at 1050 °C. Moreover, the oxidation rate shows an exponential relationship with inverse temperature ($1/T$), which matches very well with the model for diffusivity of oxidants (**Fig. S1**). The oxidation rates of the all samples can be classified into three groups, where group I is the 89 nm-thick SiC film and group II is the 394 nm- thick <111> SiC films, both LPCVD grown at low temperature. Group III is assigned to the rest four SiC films listed in Table 1. The oxidation rate of the group I (~ 42 nm/h) was almost 2.5 times higher than that of the group II (~19 nm/h), and about 4-fold compared to that of the group III. No significant difference was observed in group III, where the <111> SiC and the low-temperature LPCVD SiC films exhibit a marginally faster oxidation rate than <100> films and the high-temperature LPCVD one (Fig. 4b). The thickness of a SiC film only exhibits a marked effect on oxidation if it is smaller than a certain value where planar defect density became significant. Otherwise, the thickness-dependent wet oxidation of SiC films is less visible as found for the relatively thick SiC films ranging from ~400 nm to ~976 nm. On the other hand, the SiC films bearing a combination of the <111> surface and the low-temperature growth exhibit a significantly faster oxidation rate compared to

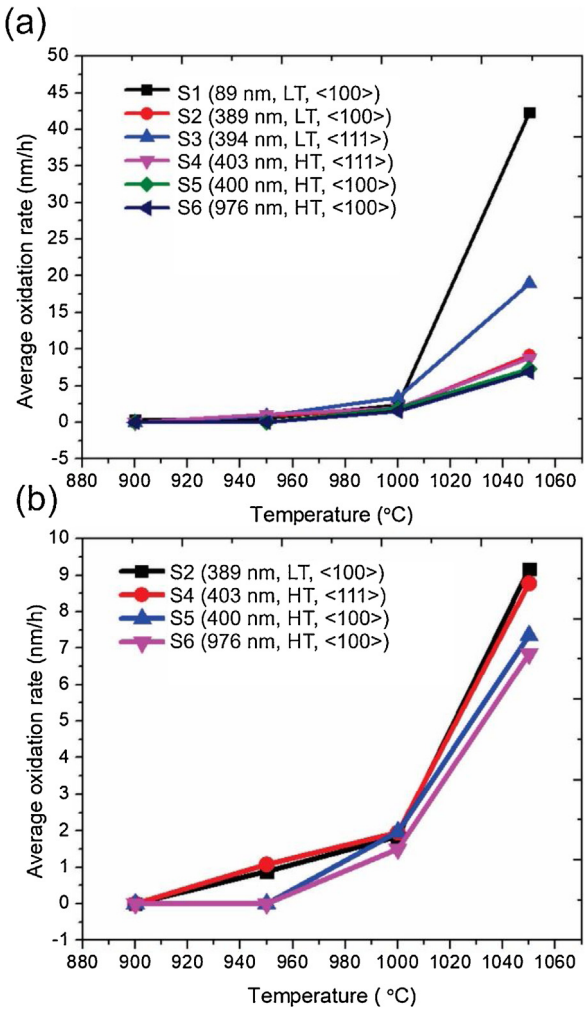


**Fig. 4.** (a) Comparing the average oxidation rates of different SiC films to identify the effects of SiC thicknesses, crystalline orientations, and growth temperature on the wet oxidation of SiC. (b) A focus on average oxidation rates of the SiC films in group 3.

that of the SiC films having either the <111> oriented surface or the low-temperature growth. These results suggest that under the tested conditions, wet oxidation of SiC mainly depends on crystalline orientations and deposition temperatures rather than their thicknesses when the SiC film thickness exceeds a certain value (e.g. above 390 nm). Determining the ratio between the volume of grown $SiO_2$ and the volume of consumed SiC is important to better understand the wet oxidation behavior. The thickness of the remaining SiC films (post oxidation) was measured using Nanometrics Nanospec reflectometer (Fig. 5a). Our experimental data shows that the variation in the thickness of the consumed SiC of different SiC films exhibits similar trends and features as observed previously for the as-grown $SiO_2$ with respect to the crystalline orientations, thickness and the grown-temperatures of the SiC films at different oxidation temperature. Detailed information on the values of the consumed SiC thickness can be found in the supporting information (**Table S1 to S4**). Notably, the volume ratios of the as-grown $SiO_2$ and consumed SiC are determined ranging from ~1.8 to ~2 at oxidation temperature of 1050 °C depending on the choice of SiC films (Fig. 5g), which is relatively close to the value of Si oxidation (2.1) [37].

Fig. 6 shows AFM images of unoxidized SiC films and the as-grown silicon oxide layer at 1000 °C. For the unoxidized SiC films, the surface morphologies strongly depend on their thicknesses and crystalline orientations (Fig. (6 a, **d, g, j**)) [44–46]. With the same <100> orientation and low LPCVD temperature, the 389-nm-thick SiC films exhibit larger crystal domains than the 89-nm-thick SiC films, while the 976-nm-thick SiC film displays the largest domain size. On the other hand, at the same thickness (~ 400 nm) and low LPCVD temperature, the <111> SiC shows flake-like surface compared to grain-like surface observed in the <100> SiC films. Although the surface roughness relatively increased, the original surface morphology of SiC are still observable in the as-grown oxide films, indicating a correlation between the surface morphology on the wet oxidation of SiC ((Fig. 6**(b, e, h, k)**). AFM images **e** and **k** clearly show increase in height of the oxidized film that correlate to the edges of the domains that indicates higher growth at these boundaries. Moreover, previous studies suggested the presence of excess carbon released during oxidation at or near the $SiO_2$/SiC interfaces, either as isolated atoms or in the form of cluster [38–41]. These residual carbon-related defects normally result in negative impacts on the electronic/electrical properties of SiC-based electronic devices [42,43]. To examine the SiC/$SiO_2$ interfaces after oxidation, we performed AFM measurements on the remaining SiC films by wet-etching the oxide layers. The AFM images showed several small, inhomogeneous protrusions on the surfaces, which can be assigned to the carbon-related particles/clusters formed after the oxidation at 1000 °C (Fig. 6**(c, f, k, l)**), consistent with the result reported by Koh et al. [41]. The AFM data of other samples oxidized at 900, 950, 1000, and 1050°C further revealed that the density of inhomogeneous particles and clusters increased with oxidation temperature. Particularly, a significant change in the surface mor-

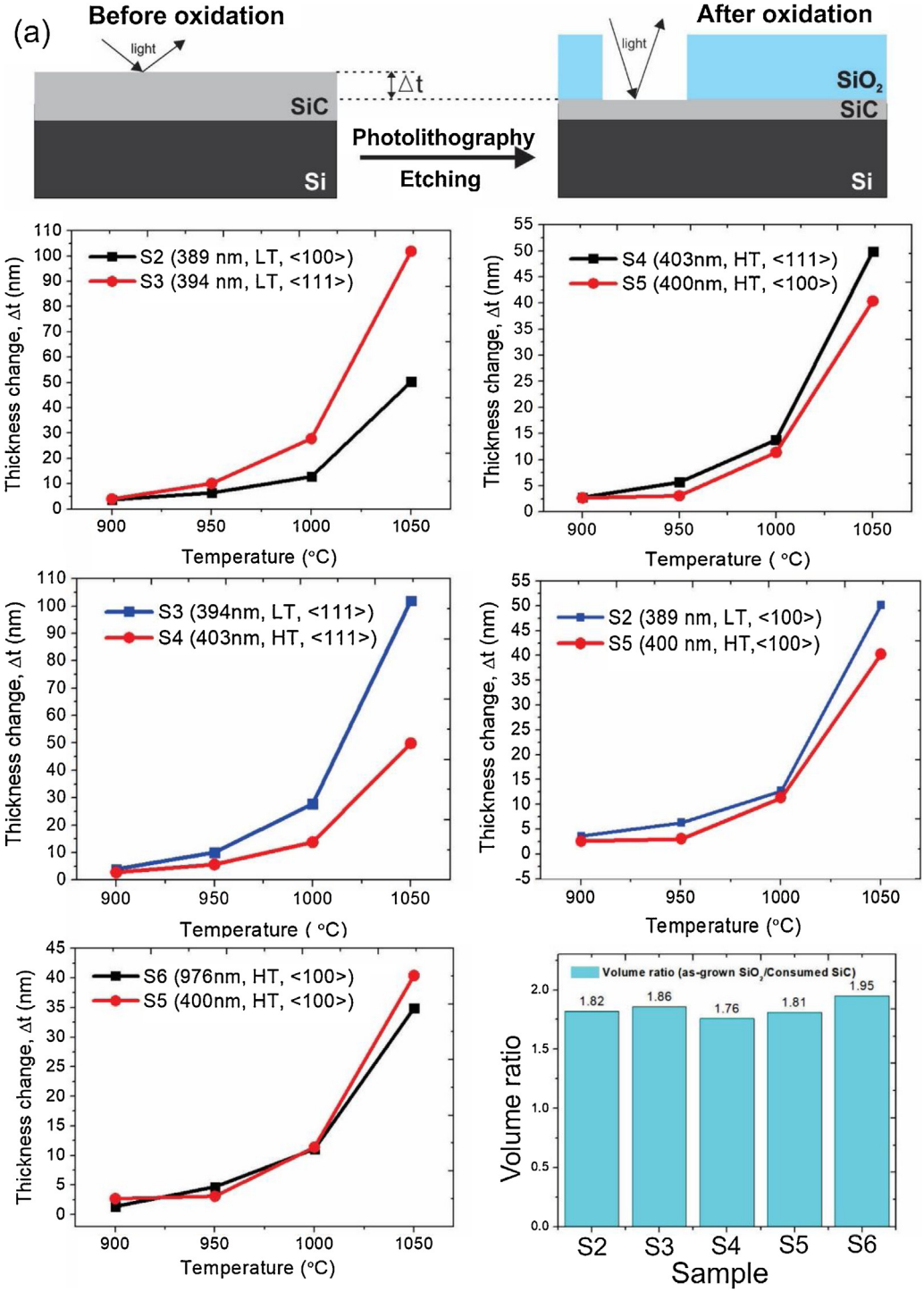


**Fig. 5.** (a) The fabrication process to determine the thickness of the consumed SiC films after wet oxidation using reflectometry measurements. (b) to (f) The dependence of the thickness of the consumed SiC films on the SiC thicknesses, growth temperature and crystalline orientations examined in the oxidation temperature ranging from 900 to 1050 °C. (g) The volume ratio of the as-grown SiC and consumed SiC for different SiC films.

phology of SiC was observed in samples oxidized at 1000 °C and 1050 °C, while there was almost no change in the films oxidized at lower temperature (e.g. 900 °C and 950 °C) (see **Fig. S2** for detailed information).

Based on the above results, we suggest that at low wet oxidation temperature (e.g. 900°C), SiC films exhibited almost the same thickness and surface morphology regardless of theirs thickness, crystal orientations, and SiC deposition temperatures. Therefore, low temperature wet oxidation can be used to exploit the selectively oxidization of Si while maintaining the physical properties of SiC. From microfabrication point of view, this feature could benefit the development of several SiC MEMS devices (e.g. the LOCOS process). To further prove this advantage, we measured the electrical properties of a 394-nm-thick SiC films before and after oxidization at 900 °C. It should be noted that the devices for electrical measurements (the inset in Fig. 7) were fabricated after the oxidation process had already been performed. To compare, we also fabricated a reference sample from the same SiC-on-Si wafer that

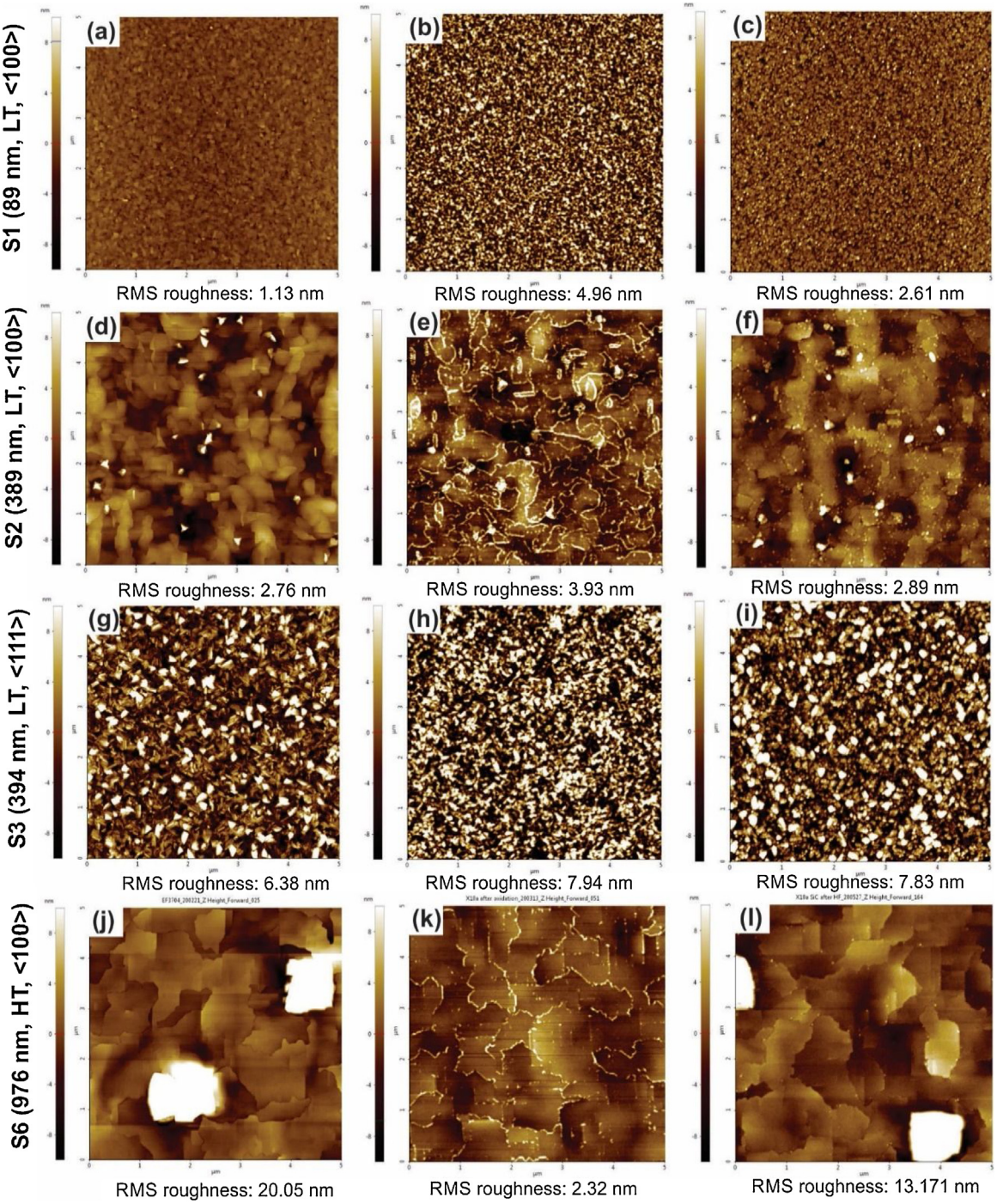


**Fig. 6.** AFM images operating in contact mode ($5 \times 5\ \mu m^2$) of ((a), (d), (g) and (j)) on different SiC films before oxidation, ((b), (e), (h) and (k)) on the as-grown $SiO_2$ of the SiC film oxidized at 1000 °C and ((c), (f), (k) and (l) exposed SiC surfaces of the SiC films oxidized at 1000 °C after removing the oxide layer by HF etching.

was not oxidized. The experimental data (on six SiC resistances for each sample) showed that the oxidation process has no negative impacts on the Ohmic contact between the electrodes and SiC films. Note that the contact resistance between Al and n-type 3C-SiC is negligible as confirmed in our previous reports [53,54]. The *I–V* characteristics (Fig. 7) show identical straight lines in the range up to 3 V, indicating stable electrical properties of oxidized SiC films subjected to 900 °C wet oxidation. The stable electrical conductivity combined with consistent material properties suggested that cubic SiC is suitable for applications operate in extreme environment (e.g. high humidity and high temperature approaching 900 °C).

## 4. Conclusion

This systematic investigation reports the effects of the crystalline orientations, thicknesses, and deposition temperature of SiC films on the wet oxidation of different SiC films heteroepitaxially deposited on Si substrates. Based on AFM and film reflectance / spectroscopic reflectometry and etched oxide thickness measurements, we observed that the crystalline orientations, thicknesses, and growth temperature of SiC films strongly influenced the wet oxidation rate. Like Si, the oxidation of <111> SiC proceeded faster than the <100> orientation. Thinner SiC films oxidized faster while thicker higher temperature deposited films were more resistant

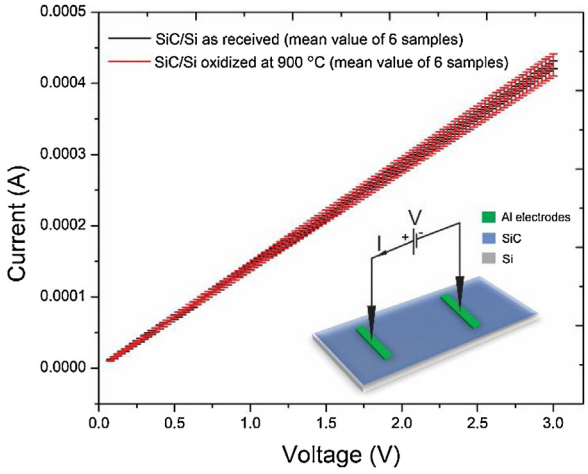


**Fig. 7.** *I-V* characteristics of the non-oxidized and oxidized 394-nm SiC film at 900 °C. The inset shows a schematic view of the device used to perform I-V characteristic measurements.

to oxidation. Moreover, domain boundaries induced higher oxidation rates for thicker films. These results indicate that wet oxidation is strongly influenced by crystal defects in the heteroepitaxial deposited films. This would imply, for the highest reliability of a 3C SiC on Si MEMS devices, the SiC surface morphology that is exposed to the harsh environment, should not have a high defect density (e.g. domain boundaries or stacking faults). Importantly, the unperturbed electrical properties of oxidized SiC confirmed by our current – voltage measurements point out that a long-term service temperature of a SiC on Si MEMS devices should be limited to 900 °C in wet environment.

## Author statement

T.A.P. performed the experiments, analyzed the experimental data, wrote the original draft and revised the manuscript. L.H., A.P. provided materials, performed AFM measurement and the oxidation process. T.-K.N., H.H. designed the masks. D.V.D., H.T., N.-T.N, H.-P.P analyzed the results. All authors discussed the results and commented on the manuscript. H.-P.P designed and directed the project.

## Declaration of Competing Interest

The authors declare that they have no known competing financial interests or personal relationships that could have appeared to influence the work reported in this paper.

## Acknowledgement

This work was partially funded by the discovery grant DE200100238 from the Australian Research Council (ARC) and performed in part at the Queensland node - Griffith - of the Australian National Fabrication Facility. A company established under the National Collaborative Research Infrastructure Strategy to provide nano and microfabrication facilities for Australia's researchers.

## Appendix A. Supplementary data

Supplementary material related to this article can be found, in the online version, at doi:https://doi.org/10.1016/j.sna.2020.112474.

## References

[1] H.-P. Phan, Y. Zhong, T.-K. Nguyen, Y. Park, T. Dinh, E. Song, R.K. Vadivelu, M.K. Masud, J. Li, M.J.A. Shiddiky, D. Dao, Y. Yamauchi, J.A. Rogers, N.-T. Nguyen, Long-lived, transfered crystalline silicon carbide nanomembranes for implantable flexible electronics, ACS Nano 13 (2019) 11572.
[2] P. Tanner, A. Iacopi, H.-P. Phan, S. Dimitrijev, L. Hold, K. Chaik, G. Walker, D.V. Dao, N.-T. Nguyen, Excellent rectifying properties of the n-3C-SiC/p-Si heterojunction subjected to high temperature annealing for electronics, MEMS, and LED applications, Sci. Rep. 7 (2017) 17734.
[3] T.-A. Pham, A. Qamar, T. Dinh, M.K. Masud, M.R.- Zadeh, D.G. Senesky, Y. Yamauchi, N.-T. Nguyen, H.-P. Phan, Nanoarchitectonics for wide bandgap semiconductor nanowires: toward the next generation of nanoelectromechanical systems for envionrmental monitoring, Adv. Sci. (2020), 2001294.
[4] T. Dinh, H.-P. Phan, T.-K. Nguyen, V. Balarishnan, H.-H. Cheng, L. Hold, A. Iacopi, N.-T. Nguyen, D.V. Dao, Unintentionally doped epitaxial 3C-SiC(111) nanothin film as material for highly sensitive thermal sensors at high temperatures, IEEE Electron Device Lett. 39 (2018) 580.
[5] T.-A. Pham, T.-K. Nguyen, R.K. Vadivelu, T. Dinh, A. Qamar, S. Yadav, Y. Yamauchi, J.A. Rogers, N.-T. Nguyen, H.-P. Phan, A versatile sacrificial layer for transfer printing of wide bandgap materials for implantable and stretchable bioelectronics, Adv. Funct. Mater. (2020), 2004655.
[6] C. Han, H. Xu, J. Xia, J.P. Ao, Ultrahigh-temperature oxidation of 4H-SiC(0001) and gate oxide reliability dependence on oxidation temperature, J. Cryst. Growth 530 (530) (2020), 125250.
[7] J. Rozen, A.C. Ahyi, X. Zhu, J.R. Williams, L.C. Feldman, Scaling between channel mobility and interface state density in SiC MOSFETs, IEEE Trans. Electron Devices 58 (2011) 3808.
[8] D. Okamoto, H. Yano, K. Hirata, T. Hatayama, T. Fuyuki, Improved inversion channel mobility in 4H-SiC MOSFETs on Si face utilizing phosphorous-doped gate oxide, IEEE Electron Device Lett. 31 (2010) 710.
[9] I. Vickridge, J. Ganem, Y. Hoshino, I. Trimaille, Growth of $SiO_2$ on SiC by dry thermal oxidation: mechanisms, J. Phys. D Appl. Phys. 40 (2007) 6254.
[10] Y. Hongli, J. Renxu, T. Xiaoyan, S. Qingwen, Z. Yuming, Effect of re-oxidation annealing process on $SiO_2$/SiC interface characteristics, J. Semicond. 35 (2014), 066001.
[11] H. Yano, F. Katafuchi, T. Kimoto, H. Matsunami, Effects of wet Oxidation/Anneal on interface properties of thermally oxidized $SiO_2$/SiC MOS system and MOSFET's, IEEE Trans. Electron Devices 46 (1999) 504.
[12] J.R. Viejo, F. Sibieude, M.T. Clavaguera-Mora, High-temperature oxidation of CVD β-SiC part II. Relation between oxygen diffusion coefficients and parabolic rate constants, J. Eur. Ceram. Soc. 13 (1994) 177.
[13] K. Kamimura, D. Kobayashi, S. Okada, T. Mizuguchi, E. Ryu, R. Hayashibe, F. Nagaune, Y. Onuma, Preparation and characterization of $SiO_2$/6H-SiC metal-insulator-semiconductor structure using TEOS as source material, Appl. Surf. Sci. 184 (2001) 346.
[14] K. Kakubari, R. Kuboki, Y. Hijikata, H. Yaguchi, S. Yoshida, Real time observation of SiC oxidation using in-situ Ellipsometer, Mater. Sci. Forum 527 (2006) 1031.
[15] Y. Song, S. Dhar, L.C. Feldman, G. Chung, J.R. Williams, Modified Deal Grove model for the thermal oxidation of silicon carbide, J. Appl. Phys. 95 (2004) 4953.
[16] T. Narushima, T. Goto, Y. Iguchi, T. Hirai, High-temperature oxidation of chemically vapor-deposited silicon carbide in wet oxygen at 1823 to 1923 K, J. Am. Ceram. Soc. 73 (1990) 3580.
[17] W.J. Lu, A.J. Steckl, T.P. Chow, W. Katz, Thermal oxidation of sputtered silicon carbide thin films, J. Electrochem. Soc. 131 (1984) 1907.
[18] E.A. Lewis, E.A. Irene, The effect of surface orientation on silicon oxidation kinetics, J. Electrochem. Soc. 134 (1987) 2332.
[19] J.R. Ligenza, Effect of crystal orientation on oxidation rates of silicon in high pressure steam, J. Phys. Chem. 65 (2011) 1961.
[20] V. Simonka, G. Nawratil, A. Hössinger, J. Weinbub, S. Selberherr, Anisotropic interpolation method of silicon carbide oxidation growth rates for three-dimensional simulation, Solid-State Electro. 135 (2017) 135.
[21] J.J. Ahn, Y.D. Jo, S.C. Kim, J.H. Lee, S.M. Koo, Crystallographic plane-orientation dependent atomic force microscopy-based local oxidation of silicon carbide, Nanoscale Res. Lett. 6 (2011) 1.
[22] K. Christiansen, R. Helbig, Anisotropic oxidation of 6H-SiC, J. Appl. Phys. 79 (1996) 3276.
[23] B.E. Deal, A.S. Grove, General relationship of the thermal oxidation of silicon, J. Appl. Phys. 36 (1965) 3770.
[24] A.G. Doncieux, O. Bahloul, C. Gault, M. Huger, T. Chotard, Investigations of SiC aggregates oxidation: influence on SiC castables refractories life time at high temperature, J. Eur. Ceram. Soc. 32 (2012) 737.
[25] R. Yao, Y. Zheng, L. Liao, R. Zhou, Z. Feng, Surface oxidation behavior in air and $O_2$-$H_2O$-Ar atmospheres of continuous freestanding SiC films derived from polycarbosilane, Ceram. Int. 44 (2018) 20974.
[26] D. Goto, Y. Hijikata, Unified theory of silicon carbide oxidation based on the Si and C emission model, J. Phys. D Appl. Phys. 49 (2016), 225103.
[27] L. Wang, S. Dimitrijev, G. Walker, J. Han, A. Iacopi, P. Tanner, L. Hold, Y. Zhao, F. Iacopi, Color chart for thin SiC films grown on Si substrates, Mater. Sci. Forum 740 (2013) 279.

[28] B. Yang, H. Zhuang, J. Li, N. Huang, L. Liu, K. Tai, X. Jiang, Defect-induced strain relaxation in 3C-SiC films grown on a (100) Si substrate at low temperature in on step, Cryst. Eng. Comm. 18 (2016) 6817.
[29] T. Hsu, L. Breaux, B. Anthony, S. Banerjee, A. Tasch, Defect microstructure in low temperature epitaxial silicon grown by RPCVD, J. Electron. Mater. 19 (1990) 375.
[30] M. Kaminska, Z. Lillental-Weber, E.R. Weber, T. George, Structural properties of As-rich GaAs grown by molecular beam epitaxy at low temperatures, Appl. Phys. Lett. 54 (1989) 1881.
[31] H.J. Gossmann, P.A. Kumar, T.C. Leung, B. Nielsen, K.G. Lynn, F.C. Unterwald, L.C. Feldman, Point defects in Si thin films grown by molecular beam epitaxy, Appl. Phys. Lett. 61 (1992) 540.
[32] G.A. Somorjai, Y. Li, Impact of surface chemistry, PNAS 108 (2011) 917.
[33] B.V. Tran, T.A. Pham, M. Grunst, M. Kivala, M. Stöhr, Surface-confined [2+2] cycloaddition towards one-dimensional polymers featuring cyclobutadiene units, Nanoscale 9 (2017) 18305.
[34] J.K. Norskov, T. Bligaard, B. Hvolbaek, F.A. Pedersen, I. Chorkendorff, C.H. Christensen, The nature of the active site in heterogeneous metal catalyst, Chem. Soc. Rev. 37 (2008) 2163.
[35] A.K. Schmid, D. Atlan, H. Itoh, B. Heinrich, T. Ichinokawa, J. Kirschner, Fast interdiffusion in thin films: scanning-tunneling-microscopy determination of surface diffusion through microscopic pinholes, Phys. Rev. B 48 (1993) 2855.
[36] L. Han, Q. Meng, D. Wang, Y. Zhu, J. Wang, X. Du, E.A. Stach, H.L. Xin, Interrogation of bimetallic particle oxidation in three dimensions at the nanoscale, Nat. Commun. 7 (2016) 13335.
[37] K. Zekentes, K. Vasilevskiy, Advancing silicon carbide electronics technology II: core technologies of silicon carbide device processing, Mater. Res. Found. 69 (2020) 63.
[38] V.R. Vathulya, D.N. Wang, M.H. White, On the correlation between the carbon content and the electrical quality of thermally grown oxides on p-type 6H-Silicon carbide, Appl. Phys. Lett. 73 (1998) 2161.
[39] V. Afanas'ev, A. Stesmans, Cl. Harris, Observation of carbon clusters at the 4H-SiC/$SiO_2$ interface, Mater. Sci. Forum 264 (1998) 857.
[40] K.C. Chang, N.T. Nuhfer, L.M. Porter, High-carbon concentrations at the silicon dioxide-silicon carbide interface identified by electron energy loss spectroscopy, Appl. Phys. Lett. 77 (2000) 2186.
[41] A. Koh, A. Kestle, C. Wright, S.P. Wilks, P.A. Mawby, W.R. Bowen, Comparative surface studies on wet and dry sacrificial thermal oxidation on silicon carbide, Appl. Surf. Sci. 174 (2001) 210.
[42] V.V. Afanas'ev, A. Stesmans, Hole traps in oxide layers thermally grown on SiC, Appl. Phys. Lett. 69 (1996) 2252.
[43] V.V. Afansa'ev, F. Ciobanu, S. Dimitrijev, G. Pensl, A. Stesmans, Band alignment and defect states at SiC/oxide interfaces, J. Phys. Condens. Matter 16 (2004) S1839.
[44] R. Anzalone, A. Severino, G. D'Arrigo, C. Bongiorno, G. Abbondanza, G. Foti, S. Saddow, F. La Via, Heteroepitaxy of 3C-SiC on different on-axis oriented silicon substrates, J. Appl. Phys. 105 (2009), 084910.
[45] L. Wang, G. Walker, J. Chai, A. Iacopi, A. Fernandes, S. Dimitrijev, Kinetic surface roughing and wafer bow control in heteroepitaxial growth of 3C-SiC on Si(111) substrates, Sci. Rep. 5 (2015) 15423.
[46] L. Wang, S. Dimitrijev, J. Han, A. Iacopi, L. Hold, P. Tanner, H.B. Harrison, Growth of 3C-SiC on 150-mm Si(100) substrates by alternating supply epitaxy at 1000 °C, Thin Solid Films 519 (2011) 6443.
[47] C.H. Lin, Oxidation of Silicon, Encyclopedia of Microfluidics and Nanofluidics, Springer, Boston, MA, 2008.
[48] H.-P. Phan, Piezoresistive Effect of p-Type Single Crystalline 3C-SiC, Springer, 2017, http://dx.doi.org/10.1007/978-3-319-55544-7, PhD thesis.
[49] F.L. Via, A. Severino, R. Anzalone, C. Bongiorno, G. Litrico, M. Mauceri, M. Schoeler, P. Schuh, P. Wellmann, From thin film to bulk 3C-SiC growth: understanding the mechanism of defects reduction, Mater. Sci. Semicond. Process. 78 (2018) 57.
[50] M. Zimbone, M. Mauceri, G. Litrico, E.G. Barbagiovanni, C. Bongiorno, F.L. Via, Protrusions reduction in 3C-SiC thin film on Si, J. Cryst. Growth 498 (2018) 248.
[51] T.A. Pham, B.V. Tran, M.T. Nguyen, M. Stöhr, Chiral selective formation of 1D polymers based on ullmann-type coupling: the role of the metallic substrate, Small 13 (2017), 1603675.
[52] D. Haasmann, S. Dimitrijev, J.S. Han, A. Iacopi, Matter. Sci. Forum 778-780 (2014) 627.
[53] A.R.M. Foisal, H.-P. Phan, T. Dinh, T.-K. Nguyen, N.-T. Nguyen, D.V. Dao, A rapid and cost-effective metallization technique for 3C–SiC MEMS using direct wire bonding, RSC Adv. 8 (2018) 15310.
[54] T. Nguyen, T. Dinh, A.R.M. Foisal, H.-P. Phan, T.-K. Nguyen, N.-T. Nguyen, D.V. Dao, Giant piezoresistive effect by optoelectronic coupling in a heterojunction, Nature Comm. 10 (2019) 1–8.

## Biographies

**Tuan-Anh Pham** received his B.E. and M.S. degrees from Hanoi University of Technology (Vietnam) and Pukyong National University (South Korea) in 2007 and 2011, respectively. Before commencing as pH.D. candidate at Queensland Micro- and Nanotechnology Centre, Griffith University, Australia in 2020, Tuan-Anh worked as a researcher in various research institutes, including University of Groningen (the Netherlands, 2011–2016), University of Erlangen-Nuremberg (Germany, 2016–2017), Institute for Basic Science (South Korea, 2017–2019) and Nanyang Technological University (Singapore, 2019–2020). His current research interest focuses on the device physics of semiconductors, epitaxial growth of 2D materials, surface science, and interfaces.

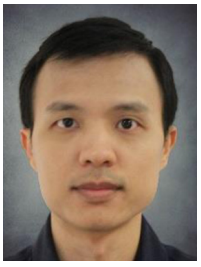

**Dr Tuan-Khoa Nguyen** is current a research fellow at Griffith University, Australia. His research interests are focused on advanced micro/nano fabrications and characterizations, semiconductor-based electronics, silicon/silicon carbide MEMS/NEMS, miniaturised sensors for manufacturing industries and bio applications. He completed his BEng and MSc degrees from Hanoi University of Science and Technology, Vietnam in 2009 and 2011, respectively. He was awarded Griffith University Postgraduate Research Scholarship (GUPRS) and Griffith University International Postgraduate Research Scholarship (GUIPRS). In 2018, he earned his PhD degree at Griffith University. He has authored and co-authored over 60 high-impact factor journal papers, several papers have been either featured in the covers of renowned journals or selected as Editor's picks. Dr Nguyen also serves as a reviewer for a number of top-ranked journals.

**Dr Han-Hao (Elliot) Cheng** is currently a research engineer at The University of Queensland, Australia. He completed his PhD from Department of Electrical and Electronic Engineering, University of Canterbury, New Zealand in 2009. Since then he has worked at The University Queensland as postdoctoral research fellow (2009–2012), and microfabrication engineer at the Australian National Fabrication Facility (2012–2017). Elliot joined the Centre for Microscopy and Microanalysis in 2017, managing the nanolithography cleanroom facility at The University of Queensland. Elliot has authored and co-authored 35 journal papers.

**Toan Dinh** is currently a lecturer at School of Mechanical and Electrical Engineering, University of Southern Queensland (USQ). Dr Dinh received his PhD in Materials Engineering from Griffith University (Australia) in 2017. His research interests include micro/nano-electromechanical systems (MEMS/NEMS), sensing technologies, sensors for harsh environments, and advanced materials for flexible and wearable applications.

**Dzung Viet Dao** received his Ph.D. degree from Ritsumeikan University, Japan in 2003. He then served as a Postdoctoral Research Fellow from 2003 to 2006, a Lecturer from 2006 to 2007, and a Chair Professor from 2007 to 2011, all at Ritsumeikan University. From 2011 A/Prof Dao joined Griffith University, Australia, where he has been teaching in Mechatronics and Mechanical Engineering. His current research interests include advanced manufacturing, MEMS sensors & actuators, transducers for harsh environments, and mechatronics/robotics.

**Hang Ta** is an Associate Professor at School of Environment and Science and Queensland Micro- and Nanotechnology Centre, Griffith University. She is a Heart Foundation Future Leader Fellow and currently leads a team of 8 students and a research fellow working on nanomaterials for diagnosis and treatment of life-threatening diseases. She got a PhD in biomaterials for drug delivery from University of Melbourne and then worked at Baker Heart and Diabetes Institute and University of Queensland before moving to Griffith University in 2020. A/Prof Ta has been awarded a number of prizes, grants and prestigious fellowships such as National Heart Foundation postdoctoral fellowship, NHMRC ECR fellowship and Heart Foundation Future Leader Fellowship. She has secured over $2.9 million ($2.7 million as CIA) in competitive grant funding from national funding agencies for both discovery and infrastructure projects. She is on Editorial Boards and is a peer reviewer for a number of journals, a chair/co-chair of conferences, serve on the committees of scientific societies, is an assessor for Masters/PhD theses, and a peer reviewer for project/fellowship applications nationally (NHMRC, Heart Foundation) and internationally (Scottish Government, French Research National Agency).

**Nam-Trung Nguyen** received his Dipl-Ing, Dr Ing, and Dr Ing Habil degrees from Chemnitz University of Technology, Germany, in 1993, 1997, and 2004, respectively. From 1999–2013 he has been an Associate Professor with Nanyang Technological University in Singapore. Since 2013, he has been serving as a Professor and the Director of Queensland Micro and Nanotechnology Centre of Griffith University, Australia. He is a Fellow of ASME and a Senior Member of IEEE. His research is focused on microfluidics, nanofluidics, micro/ nanomachining technologies, micro/nanoscale science, and instrumentation for biomedical applications. One of his current research interests is developing flexible and stretchable systems with bio interface.

**Hoang-Phuong Phan** received the B.E and M.E. from The University of Tokyo, Japan and the Ph.D. from Griffith University, Australia. He is currently is an ARC DECRA Fellow at the Queensland Micro and Nanotechnology Centre, Griffith University. His research interests include MEMS/NEMS, integrated sensors, flexible/implantable electronics, and bio-sensing applications. Dr. Phan was a visiting scholar at Stanford University, CA, USA in 2017, and Northwestern University, IL, USA in 2019. He has published over 80 journal articles, two US patents, and two book/book-chapters. Dr. Phan was honoured with the MEXT scholarships, GU publication award, the GGRS-IEIS travel grant, the Springer outstanding theses award, the Australian Nanotechnology Network Overseas Fellowship, GU Postdoctoral Fellowship, ARC DECRA, and Pro Vice Chancellor Excellent Early Career Researcher. He has served on the technical program committee of the International Conference on Micro Electro Mechanical Systems (IEEE MEMS).